Contract No.:

This manuscript has been authored by Savannah River Nuclear Solutions (SRNS), LLC under Contract No. DE-AC09-08SR22470 with the U.S. Department of Energy (DOE) Office of Environmental Management (EM).

SRNL-STI-2017-00551

MODELING OF SELF-HEATING IN ANION EXCHANGE COLUMNS FOR PLUTONIUM RECOVERY

Dr. James E. Laurinat
Savannah River National Laboratory
Aiken, South Carolina

Abstract

A finite element code has been developed to model radiolytic self-heating in anion exchange columns. Anion exchange columns are used to extract plutonium from nitric acid solutions as part of the Purex process. When columns are used to extract Pu-238, significant rates of radiolytic heating pose a risk that column temperatures could rise to the point where a runaway resin degradation reaction occurs. A runaway degradation reaction can lead to a potentially violent thermal excursion, where gas generation from the degradation reaction causes the column to eruct. The finite element code focuses on predicting the maximum temperature due to radiolytic heating in order to ensure that this maximum temperature remains below the temperature required to initiate a reaction excursion. The code also can be used to calculate the cumulative radiological dose to the resin.

The finite element code calculates concentration profiles and temperatures for normal operation of a column, including loading, washing, and elution of the resin, and for natural circulation during flow stoppages. Resin loading is modeled by combining a chemical equilibrium absorption relation with models for axial dispersion and solid phase diffusion. Desorption is modeled by combining the axial dispersion model with a shrinking core diffusion model. Natural convection calculations are based on the Ergun relation for flow in a packed bed, using pressure gradients obtained from temperature and composition differences in the column solution.

The model was applied to calculate maximum temperatures in anion exchange columns used to extract Pu-238 for the Cassini mission at the Savannah River Site (SRS) and for a Pu-238 laboratory-scale column at Los Alamos National Laboratory (LANL). More recently, the model was used to predict doses to the resin for feeds containing plutonium, americium, and curium. For this calculation, it was assumed that the resin absorbs plutonium much more strongly than either americium or curium. Results are presented for all three studies.

Nomenclature

C_{Pu}	total plutonium concentration adsorbed on the resin, in resin pores, and in the bulk solution, kg/m^3
c	fractional concentration of elution acid (250 mol/m^3), dimensionless
$c_{p,f}$	solution heat capacity, J/kg/K
$c_{p,bed}$	bulk heat capacity for the resin bed, J/kg/K
D_i	distribution coefficient for ith element with respect to Pu
D_{mix}	dispersion coefficient for mixing due to density gradients, m^2/s
D_{part}	particle diffusivity for diffusion of Pu in the resin bead, m^2/s

D_{pore}	bulk pore diffusivity for diffusion of Pu in the resin bead, normalized to account for differences between solid and solution concentrations, m^2/s
D'_{pore}	bulk pore diffusivity for diffusion of Pu in the resin bead, m^2/s
d	column diameter, m
d_p	average resin bead diameter, m
f	bulk concentration of plutonium adsorbed onto the resin, kg/m^3
f_{feed}	bulk concentration of plutonium adsorbed onto the resin when the resin is fully loaded, kg/m^3
f_0	bulk concentration of plutonium adsorbed onto the resin at the end of the decon wash, kg/m^3
G	during loading, bulk rate of transfer of plutonium from bulk solution to the resin, $kg/m^3/s$
G_a	during elution, bulk rate of transfer of plutonium from the resin to the bulk solution due to desorption, $kg/m^3/s$
G_b	during elution, bulk rate of diffusion of plutonium from the bulk solution to the resin pore solution, $kg/m^3/s$
g	gravitational acceleration, m/s^2
K_1	equilibrium constant for the solubility of plutonium from nitric acid solutions on Ionac 641 resin, (mol/m^3)
k_{bed}	bulk thermal conductivity for the resin bed, J/m/s/K
Q_{decay}	mass rate of heat generation due to radioactive decay of plutonium isotopes, W/kg
R	column radius, m
R_p	average resin bead radius, m
$R_{p,1}$	during elution, radius of the undesorbed core of resin bead, m
r	radial distance from the center of the column, m
r_p	radial distance from the center of the resin bead, m
T	bulk temperature, K
t	time for heat transfer and mass transfer to bulk solution, s
t'	characteristic time for adsorption with continuous contact between the loading solution and the resin bead surfaces, s
t_p	time for adsorption within a resin bead, s
$\langle t_p \rangle$	average residence time for adsorption at a given axial level, s
$t_{p,a}$	time for desorption within a resin bead, s
$\langle t_{p,a} \rangle$	average residence time for desorption at a given axial level, s
$t_{p,b}$	time for interchange between the bulk solution and resin bead pores, s
$\langle t_{p,b} \rangle$	average residence time for interchange between the bulk solution and resin bead pores at a given axial level, s

v_c	characteristic velocity for axial mixing due to density gradients, m/s
$v_{c,eff}$	effective velocity for density gradient mixing, m/s
v_r	superficial radial velocity in the column, m/s
v_z	superficial axial velocity going from the top to the bottom of the column, m/s
x	during loading and the decon wash, bulk concentration of plutonium in the bulk solution, kg/m^3
x_a	during desorption, local concentration of plutonium in the resin bead pores, kg/m^3
x_{feed}	concentration of plutonium in the feed solution, kg/m^3
x_{max}	maximum plutonium concentration in the bulk solution, kg/m^3
x_{sat}	plutonium concentration in the bulk solution at saturation, kg/m^3
y	during elution, bulk concentration of plutonium in the resin bead pores due to diffusion from the bulk solution, kg/m^3
$\bar{y}$	during desorption, concentration of plutonium in the pores at the resin bead surface, kg/m^3
z	axial distance from the top of the resin bed, m
z_0	axial location at which the dispersion coefficient for density gradient mixing is evaluated, m
α_r	radial dispersion coefficient, m^3/s
α_z	axial dispersion coefficient, m^3/s
ε_i	volume fraction of column occupied by liquid in interparticle space
$\varepsilon_{i,1}$	fraction of the total resin bed volume occupied by the resin bead pores before desorption of plutonium, dimensionless
$\varepsilon_{i,2}$	fraction of the total resin bed volume occupied by the resin bead pores after desorption of plutonium, dimensionless
$\varepsilon_{i,2,0}$	fraction of the total resin bed volume occupied by the resin bead pores after all plutonium has desorbed, dimensionless
ε_o	fraction of the total resin bed volume occupied by the bulk solution, dimensionless
η	factor to account for the difference between the pseudo-steady-state shrinking core approximation and the exact shrinking core model solution for the total desorption time, dimensionless
μ	solution dynamic viscosity, kg/m/s
ρ_f	solution density, kg/m^3
$\bar{\rho}_f$	average solution density at a given axial level, kg/m^3
ρ_{bed}	bulk density of the resin bed, kg/m^3
τ_{part}	time for a resin bead to become fully loaded with plutonium due to particle diffusion, s
τ_{pore}	time for complete desorption of a resin bead by pore diffusion, s

Introduction

The original impetus to develop a model for the recovery of plutonium in anion exchange columns was to assess the change in column temperatures for increased plutonium loading on the column. Historically, at SRS, an anion exchange column was used to recover and recycle Pu-238 from scrap solutions. When recovery of Pu-238 to make product for the Cassini mission was started, an increase in column loading was desired. (The Cassini mission was a joint endeavor of the National Aeronautics and Space Administration (NASA), the European Space Agency (ESA), and the Italian space agency Agenzia Spaziale Italiana (ASI), to explore Saturn and its moons. Pu-238 was used in radioisotope thermoelectric generators (RTGs) to power the Cassini satellite.)

The Pu-238 column load was limited to prevent thermal degradation and disintegration of the resin bed. At low temperatures, resin bed temperatures increase primarily due to decay heat from Pu-238. At temperatures exceeding about 388 K, an exothermic reaction between nitric acid and resin predominates. This reaction causes a potentially violent temperature excursion. Operating limits stipulated a maximum column temperature of 333 K to protect against the exothermic nitric acid-resin reaction.

The greatest potential for a resin bed temperature excursion occurs during flow interruptions. If the flow is stopped during loading, washing, or elution, the temperature rises due to heat from the decay of Pu-238 until conditions for a temperature excursion are met. The temperature rise is nearly adiabatic; calculations showed that natural convection to the ambient air is not effective in cooling the resin bed.

The original model evaluated the effects of increases in column loading on column temperatures during flow interruptions, as a function of time, for a uniform velocity flow through the column.[1] Subsequently, at the request of Los Alamos National Laboratory, the model was extended to include natural convection in order to model temperature increases inside a column during a flow stoppage.[2,3,4] Finally and more recently, the original, one-dimensional flow model was coupled with a dose calculation to estimate the total dose to the resin for a feed containing plutonium, americium, and curium, along with cesium and strontium fission products.

The following sections describe the mass transfer model, which was developed for one-dimensional uniform flow, and the heat transfer aspects of the natural convection model for the resin bed, which is applied assuming two-dimensional axisymmetric flow. Results from both the mass and heat transfer calculations are reported. The mass transfer and heat transfer model descriptions are followed by a brief overview of the resin dose calculation.

Mass Transfer Model

Ion Exchange Chemistry

In the ion exchange column, plutonium is selectively adsorbed on an anionic resin from an 8000 mol/m^3 HNO_3 solution and is eluted with 250 mol/m^3 HNO_3. Historically, plutonium ion exchange columns used Dowex-1™ X-4 ion exchange resin. At the time the original model was developed, the column used Ionac 641™ macroporous resin converted to a nitrate form. Later, both the LANL laboratory-scale column and the SRS mixed actinide ion exchange column

™ Dowex-1 is a registered trademark of DowDuPont of Midland, Michigan.
™ Ionac 641 is a registered trademark of LANXESS Sybron Chemicals, Inc., of Birmingham, New Jersey.

used Reillex HPQ™ pyridine-based resin. For all three resins, the following reaction occurs on the resin surfaces,[5] which are assumed to be evenly distributed throughout the resin beads.

$$R_2Pu(NO_3)_6\,(solid) \Leftrightarrow PuNO_3{}^{3+}(aq) + 3NO_3{}^{-}(aq) + 2RNO_3(solid)$$

where R denotes a chemically active site on the resin substrate.

Equilibrium solution concentrations were calculated by combining the solubility product $K_1 = \left[PuNO_3{}^{3+}\right]\left[NO_3{}^{-}\right]^3$ with the equilibrium product for the aqueous phase complexation reaction[5]

$$Pu^{4+}(aq) + NO_3{}^{-}(aq) \Leftrightarrow PUNO_3{}^{3+}(aq)$$

The solubility product depends on the type of resin. Figure 1 depicts the solubility as a function of nitric acid concentration for both Dowex-1™ and Ionac 641™.

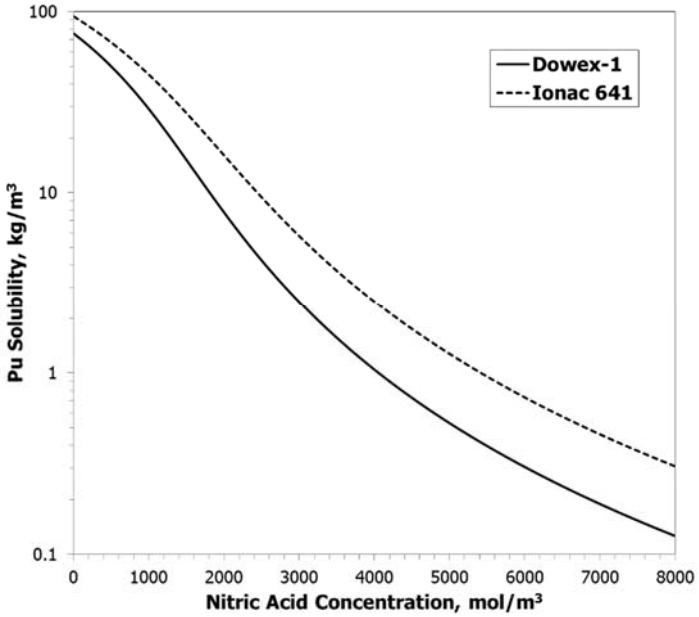

Figure 1. Saturated Equilibria for Dowex-1™ and Ionac 641™ Resins in Nitric Acid

Mass Transfer Model Development

Separate mass transfer models were developed for loading and washing and for elution. Both models use one-dimensional, transient mass conservation equations, with explicit terms to account for adsorption or elution of plutonium into or out of the resin beads. These models divide the total plutonium concentration, C_{Pu}, into a bulk flow concentration, x, a resin bead pore solution concentration, y, and an adsorbed concentration, f:

$$C_{Pu} = x + y + f \qquad (1)$$

All concentrations are based on the bulk volume of the resin bed.

™ Reillex HPQ is a registered trademark of Vertellus Specialty Chemicals, Inc., of Indianapolis, Indiana.

Adsorption Mass Transfer

The mass balances for adsorption and washing take the form

$$\frac{\partial x}{\partial t} = -v_z \frac{\partial x}{\partial z} + \alpha_z \frac{\partial^2 x}{\partial z^2} \tag{2}$$

and

$$\frac{\partial f}{\partial t} = G \tag{3}$$

The axial dispersion coefficient is calculated using a mixing length of two bead diameters.[6] This gives

$$\alpha_z = 2 d_p v_z \tag{4}$$

Diffusion to the resin bead surfaces controls the rates of adsorption and elution. Because the plutonium ionic species react rapidly at the resin surface, adsorption takes place at the outer surfaces of the resin beads before the plutonium can penetrate to the interior of the beads. Consequently, solid-phase, or particle, diffusion controls the rate of adsorption.[5] The particle diffusion model is analogous to a molecular diffusion model, with a particle diffusivity and the bulk adsorbed concentration replacing the ordinary diffusivity and the solution concentration.

An approximate solution for diffusion through a spherical particle is[7]

$$\frac{t_p}{\tau_{part}} = -ln\left(1 - \left(\frac{f}{f_{feed}}\right)^2\right) \tag{5}$$

where

$$\tau_{part} = \frac{{d_p}^2}{4\pi^2 D_{part}} \tag{6}$$

The variable t_p represents the time needed for a single resin bead to adsorb a given amount of plutonium. The collective adsorption time for resin beads at a particular bed level, $\langle t_p \rangle$, is an average of these individual adsorption times, weighted by the adsorbed fraction f. The integral representation of this weighted average is:

$$\langle t_p \rangle = \frac{f_{feed}}{f} \int_0^{t_p} \frac{f}{f_{feed}} dt_p \tag{7}$$

The time required for the loading calculation is the average time it takes for a level of the resin bed to adsorb plutonium. The calculation of this loading time is based on the stipulation that the loading profile is fully developed. If the resin beads are in continuous contact with the loading solution, then, for a fully-developed profile, the average adsorption time $\langle t_p \rangle$ and the loading time t' are related by the characteristic equation,

$$\langle t_p \rangle \Delta f = f \Delta t' \tag{8}$$

At the loading front, however, only a portion of the bulk solution is in saturated equilibrium with the adsorbed plutonium on the resin surfaces. The mixing of saturated and unsaturated solution occurs at a macroscopic rather than a molecular level, because axial dispersion predominates over molecular diffusivity.

Consequently, this mixing can be modeled by assuming that the bulk flow is segregated into one fraction that contains dissolved plutonium and another that does not. Under this assumption, the actual loading time, t, and the loading time for continuous contact, t', are related by

$$\Delta t' = \frac{x}{x_{feed}} \Delta t \tag{9}$$

The preceding equations combine to yield the following expression for the loading mass transfer rate

$$G = f_{feed} \frac{x}{x_{feed}} \frac{\left(\frac{f}{f_{feed}}\right)^2}{ln\left(\frac{f_{feed}+f}{f_{feed}-f}\right) - 2\frac{f}{f_{feed}}} \frac{1}{\tau_{part}} \tag{10}$$

As $f \to 0$,

$$G = f_{feed} \frac{x}{x_{feed}} \frac{1.5 f_{feed}}{f} \frac{1}{\tau_{part}} \tag{11}$$

Elution Mass Transfer

During elution, dilute acid diffuses inward from the resin bead surface to displace more concentrated acid, and plutonium nitrate species diffuse outward toward the surface. Thus, the acid concentration increases and the plutonium nitrate concentration decreases going toward the center of the bead. This implies that a saturated plutonium nitrate solution exists at only one radial location within the bead, provided the adsorbed plutonium concentration is sufficient to locally saturate the pore solution. Plutonium nitrate species diffuse outward from this surface.

The mass balances for elution are:

$$\frac{\partial c}{\partial t} = \frac{\varepsilon_o}{\varepsilon_o + \varepsilon_{i,1}} \left(-v_z \frac{\partial c}{\partial z} + \alpha_z \frac{\partial^2 c}{\partial z^2} \right) \tag{12}$$

$$\frac{\partial x}{\partial t} = -v_z \frac{\partial x}{\partial z} + \alpha_z \frac{\partial^2 x}{\partial z^2} + G_a - G_b \tag{13}$$

$$\frac{\partial f}{\partial t} = -G_a \tag{14}$$

and

$$\frac{\partial y}{\partial t} = G_b \tag{15}$$

where c is the fraction of the bulk solution that is 250 mol/m^3 elution acid, G_a is the rate of plutonium desorption, and G_b is the rate of diffusion of plutonium from the bulk solution into desorbed resin beads. The factor $\frac{\varepsilon_o}{\varepsilon_o + \varepsilon_{i,1}}$, which is the ratio of the bulk solution volume to the total solution volume before desorption, accounts for interchange of elution acid between the bulk and pore solutions. Use of this factor is based on a quasi-equilibrium approximation. In other words, diffusion of nitric acid is assumed to be rapid compared with diffusion of plutonium nitrate species, so that the pore and bulk solution nitric acid concentrations are equal while plutonium diffuses.

Separate rate models are used for desorption and interchange of plutonium between the bulk and pore solutions, because the desorption model transfers plutonium directly from the adsorbed solid to the bulk solution, without allowing for any plutonium in the pore volume. A shrinking core approximation describes desorption of plutonium from the resin beads.[5]

If the pore diffusivity is assumed to be constant, the pore diffusion equation becomes

$$\frac{\partial x_a}{\partial t_{p,a}} = \frac{D'_{pore}}{r_p{}^2} \frac{\partial}{\partial r_p}\left(r_p{}^2 \frac{\partial x_a}{\partial r_p} \right) \tag{16}$$

A pseudo-steady approximation is applied to eliminate time dependent terms:

$$\frac{d}{dr_p}\left(r_p{}^2 \frac{dx_a}{dr_p} \right) = 0 \tag{17}$$

The steady-state approximation is valid, provided that the concentration of plutonium adsorbed on the surface is greater than the bulk concentration in a solution in saturated equilibrium with the adsorbed plutonium. Errors introduced by this approximation are accounted for later in this derivation.

Equation 16 is solved with the boundary conditions

$$x_a = x_{max} \text{ at } r_p = R_{p,1} \tag{18}$$

and $$x_a = 0 \text{ at } r_p = R_p \tag{19}$$

The pseudo-state-state solution is

$$x_a = x_{max} \frac{R_{p,1}\left(R_p - r_p\right)}{r_p\left(R_p - R_{p,1}\right)} \tag{20}$$

This solution is useful only when expressed in terms of a fractional desorption. To convert this result to a useful form, a mass balance is applied to equate the shrinkage of the undissolved core region with the diffusion rate at the bead surface. This takes the form

$$4\pi R_p{}^2 D'_{pore} \left.\frac{dx_a}{dr_p}\right|_{r_p = R_p} = f_0 \frac{d}{dt_p}\left(\frac{4}{3}\pi R_{p,1}{}^3 \right) \tag{21}$$

The initial condition for this equation is

$$R_{p,1} = R_p \text{ when } t_{p,a} = 0, \tag{22}$$

and the final condition is

$$R_{p,1} = 0 \text{ when } t_{p,a} = \tau_{pore} \tag{23}$$

The fractional desorption is defined by

$$\frac{f}{f_0} = \left(\frac{R_{p,1}}{R_p} \right)^3 \tag{24}$$

Solution of the preceding equations yields the following expression for the rate of desorption during elution:

$$\frac{t_{p,a}}{\tau_{pore}} = 1 + 2\frac{f}{f_0} - 3\left(\frac{f}{f_0} \right)^{\frac{2}{3}} \tag{25}$$

where

$$\tau_{pore} = \frac{d_p{}^2 f_0}{24 D'_{pore} x_{max}} \tag{26}$$

A modified pore diffusivity is defined to incorporate differences between the adsorbed solid and saturated solution concentrations of plutonium:

$$D_{pore} = \frac{D'_{pore} x_{max}}{f_0} \tag{27}$$

In terms of this modified diffusivity,

$$\tau_{pore} = \frac{d_p{}^2}{24 \eta D_{pore}} \tag{28}$$

An effectiveness factor η of 0.75 was added to this equation to account for errors introduced by the pseudo-state-state approximation.

As in the adsorption rate analysis, the collective adsorption time for resin beads at a particular bed level, $\langle t_{p,a} \rangle$, is calculated as a weighted average of individual adsorption times, $t_{p,a}$, from the integral,

$$\langle t_{p,a} \rangle = \frac{f_0}{f} \int_0^{t_{p,a}} \frac{f}{f_0} dt_{p,a} \tag{29}$$

This integral gives

$$\frac{\langle t_{p,a} \rangle}{\tau_{pore}} = \frac{f}{f_0} - \frac{6}{5}\left(\frac{f}{f_0}\right)^{\frac{2}{3}} + \frac{f_0}{5f} \tag{30}$$

The expression for the rate of desorption is obtained by differentiating Equation 30. This gives

$$\frac{1}{f_0}\frac{df}{d\langle t_{p,a} \rangle} = \frac{1}{\tau_{pore}\left(1 - \frac{4}{5}\sqrt[3]{\frac{f_0}{f}} - \frac{1}{5}\left(\frac{f_0}{f}\right)^2\right)} \tag{31}$$

Equation 31 gives the collective rate of desorption for resin beads continuously in contact with a bulk solution of 250 mol/m^3 elution acid that does not contain plutonium. Correction factors must be added to account for variations in acid and plutonium concentrations in the bulk solution. To derive a correction factor for acid concentration, it is assumed that during desorption the bulk flow is segregated into one fraction, c, that contains dilute elution acid (250 mol/m^3) and another, $1-c$, that contains wash acid (8000 mol/m^3). This implies that changes in the collective desorption time and the elapsed time are related by

$$\Delta\langle t_{p,a} \rangle = c\Delta t \tag{32}$$

To correct Equation 31 for the plutonium concentration gradient, the average plutonium concentration in the pores at the resin bead surface, y, must be calculated. This concentration is obtained from a quasi-equilibrium relation, in which the rate of diffusion of plutonium to the bulk solution varies about a mean of zero. To derive this relation, it is assumed that the elution

acid is poorly mixed in the bulk solution, so that it segregates into a fraction $\frac{x}{x_{max}}$ that is in saturated equilibrium with the adsorbed plutonium and a fraction $c - \frac{x}{x_{max}}$ that contains no plutonium. It follows that, if the diffusion resistance of the bulk solution is negligible, plutonium diffuses into the resin bead from a saturated bulk solution a fraction of time $\frac{x}{x_{max}}$ and diffuses from the resin bead into elution acid that contains no plutonium a fraction of time $c - \frac{x}{x_{max}}$. The quasi-equilibrium relation is obtained by integrating the transient diffusion equation. Such an integration shows that the mass transfer is proportional to the concentration difference and the square root of the contact time. In this instance, then,

$$\left(x_{max} - \bar{y}\right)\sqrt{\frac{x}{x_{max}}} - \bar{y}\sqrt{c - \frac{x}{x_{max}}} = 0 \tag{33}$$

Solution of this equation gives the concentration gradient correction factor,

$$1 - \frac{\bar{y}}{x_{max}} = \frac{\sqrt{c - \frac{x}{x_{max}}}}{\sqrt{\frac{x}{x_{max}}} + \sqrt{c - \frac{x}{x_{max}}}} \tag{34}$$

The mass transfer rate for desorption, including the correction factors for the acid concentration and the plutonium concentration gradient, is

$$G_a = -\left(1 - \frac{\bar{y}}{x_{max}}\right)\frac{df}{d\left\langle t_{p,a}\right\rangle}\frac{d\left\langle t_{p,a}\right\rangle}{dt} \tag{35}$$

Evaluation of Equation 35 yields the rate expression,

$$G_a = \frac{-cf_0\left(\frac{\sqrt{c - \frac{x}{x_{max}}}}{\sqrt{\frac{x}{x_{max}}} + \sqrt{c - \frac{x}{x_{max}}}}\right)}{\tau_{pore}\left(1 - \frac{4}{5}\sqrt[3]{\frac{f_0}{f}} - \frac{1}{5}\left(\frac{f_0}{f}\right)^2\right)} \tag{36}$$

The desorption model does not account for diffusion of plutonium into and out of the resin bead pores as the elution concentration spike travels down the column. The diffusion equation for this interchange is based on the approximate solution for particle diffusion in a sphere,[5] which uses a quadratic concentration gradient. Similarly, pore diffusion between the bulk and pore solutions is modeled with quadratic gradients. Based on the assumption that the bulk solution is poorly mixed at the molecular level, it is assumed that the bulk solution is segregated into one volume fraction in which the plutonium concentration is in saturated equilibrium with the adsorbed plutonium and another that does not contain any plutonium. The net diffusion for such a segregated mixture can be expressed by

$$\frac{1}{{\varepsilon_{i,2}}^2}\frac{dy^2}{dt_{p,b}} = \frac{1-\varepsilon_o}{\varepsilon_{i,2}}\frac{4\pi^2 D_{pore}}{{d_p}^2}\left(\frac{x}{x_{max}}\left(\left(\frac{x_{max}}{\varepsilon_o}\right)^2 - \left(\frac{y}{\varepsilon_{i,2}}\right)^2\right) - \left(1-\frac{x}{x_{max}}\right)\left(\frac{y}{\varepsilon_{i,2}}\right)^2\right) \quad (37)$$

This simplifies to

$$\frac{1}{{\varepsilon_{i,2}}^2}\frac{dy^2}{dt_{p,b}} = \frac{1-\varepsilon_o}{\varepsilon_{i,2}}\frac{4\pi^2 D_{pore}}{{d_p}^2}\left(\frac{x_{max}x}{{\varepsilon_o}^2} - \frac{y^2}{{\varepsilon_{i,2}}^2}\right) \quad (38)$$

where the pore liquid concentration is based on the volume fraction in the pores of the eluted portion of the resin beads, $\varepsilon_{i,2}$ The factor $\frac{1-\varepsilon_o}{\varepsilon_{i,2}}$ appears because the pore plutonium concentration is normalized with respect to the pore volume, whereas the pore diffusivity applies to the entire resin bead volume.

The eluted pore volume fraction is related to the pore volume in a completely eluted bead, $\varepsilon_{i,2,0}$, by

$$\varepsilon_{i,2} = \left(1-\frac{f}{f_0}\right)\varepsilon_{i,2,0} \quad (39)$$

The initial loading has been used in place of the full equilibrium loading in this calculation, because it gives the correct initial condition: i.e., the eluted pore volume fraction must be zero at the beginning of the elution.

Time variations of the eluted pore volume fraction have been neglected in Equation 38. This simplification does not introduce significant errors, since the rate of desorption is slower than the rate of interdiffusion of plutonium between the pores and the bulk liquid.

The collective adsorption time for resin beads at a particular bed level, $\langle t_{p,b}\rangle$, is calculated as a weighted average of individual adsorption times, $t_{p,b}$,from the integral,

$$\langle t_{p,b}\rangle = \frac{f_0}{f}\int_0^{t_{p,b}}\frac{f}{f_0}dt_{p,b} \quad (40)$$

Solution of this integral gives

$$\langle t_{p,b}\rangle = \frac{{d_p}^2}{4\pi^2 D_{pore}\varepsilon_{i,2}(1-\varepsilon_o)}\left(\frac{\varepsilon_{i,2}\sqrt{x_{max}x}}{\varepsilon_o y}\ln\left(\frac{\frac{\sqrt{x_{max}x}}{\varepsilon_o}+\frac{y}{\varepsilon_{i,2}}}{\frac{\sqrt{x_{max}x}}{\varepsilon_o}-\frac{y}{\varepsilon_{i,2}}}\right) - 2\right) \quad (41)$$

The expression for the rate of desorption is obtained by differentiating Equation 41 to get

$$\frac{dy}{d\langle t_b \rangle} = \frac{4\pi^2 D_{pore}(1-\varepsilon_o)\left(\frac{y^2}{{\varepsilon_{i,2}}^2}\right)\left(\frac{x_{max}x}{{\varepsilon_o}^2} - \frac{y^2}{{\varepsilon_{i,2}}^2}\right)}{{d_p}^2\left(2\frac{x_{max}xy}{{\varepsilon_o}^2\varepsilon_{i,2}} - \frac{\sqrt{x_{max}x}}{\varepsilon_o}\left(\frac{x_{max}x}{{\varepsilon_o}^2} - \frac{y^2}{{\varepsilon_{i,2}}^2}\right) ln\left(\frac{\frac{\sqrt{x_{max}x}}{\varepsilon_o} + \frac{y}{\varepsilon_{i,2}}}{\frac{\sqrt{x_{max}x}}{\varepsilon_o} - \frac{y}{\varepsilon_{i,2}}}\right)\right)} \quad (42)$$

The mass transfer rate is expressed in terms of the actual elapsed time, so that

$$G_b = \frac{dy}{d\langle t_{p,b} \rangle}\frac{d\langle t_{p,b} \rangle}{dt} \quad (43)$$

Changes in the time for diffusion interchange equal changes in the actual elapsed time, $\Delta\langle t_{p,b} \rangle = \Delta t$, so that

$$G_b = \frac{4\pi^2 D_{pore}(1-\varepsilon_o)\left(\frac{y^2}{{\varepsilon_{i,2}}^2}\right)\left(\frac{x_{max}x}{{\varepsilon_o}^2} - \frac{y^2}{{\varepsilon_{i,2}}^2}\right)}{{d_p}^2\left(2\frac{x_{max}xy}{{\varepsilon_o}^2\varepsilon_{i,2}} - \frac{\sqrt{x_{max}x}}{\varepsilon_o}\left(\frac{x_{max}x}{{\varepsilon_o}^2} - \frac{y^2}{{\varepsilon_{i,2}}^2}\right) ln\left(\frac{\frac{\sqrt{x_{max}x}}{\varepsilon_o} + \frac{y}{\varepsilon_{i,2}}}{\frac{\sqrt{x_{max}x}}{\varepsilon_o} - \frac{y}{\varepsilon_{i,2}}}\right)\right)} \quad (44)$$

As $\frac{y}{\varepsilon_{i,2}} \to \frac{\sqrt{x_{max}x}}{\varepsilon_o}$, this reduces to

$$G_b = \frac{4\pi^2 D_{pore}(1-\varepsilon_o)}{{d_p}^2}\left(\frac{\sqrt{x_{max}x}}{\varepsilon_o} - \frac{y}{\varepsilon_{i,2}}\right) \quad (45)$$

Comparison of Mass Transfer Model Predictions with Measurements

Model predictions were compared with a previously measured column loading profile and with results from two laboratory-scale test elutions. In the first elution, a short 0.092-m column was nearly fully loaded with plutonium. Results from this elution and the measured profile were used to determine the saturated equilibrium plutonium concentration, the maximum plutonium loading, and the particle diffusivity. The second elution, in which a longer 0.375-m column was partially loaded, approximated conditions in the production column. Results from both elutions were used to estimate the pore diffusivity and volume fractions for the bulk and pore solutions.

The loading, washing, and elution times for the second test elution were shortened so that this elution could be completed in one working day. Although this test was abbreviated, the elution time was sufficient to allow removal of most of the plutonium from the column. During typical column elutions, the head cut takes 1.2 bed volumes, the heart cut takes 1.5 bed volumes, and the tail cut takes 1.9 bed volumes. The total elution volume for the second test elution was approximately equal to the head plus heart cuts for typical column operation.

Figure 2 compares measured and predicted loading profiles. A particle diffusivity of 2E-13 m^2/s was used to fit the reported data. This diffusivity is the same magnitude as that measured for Dowex™ X-8 resin.[5]

From the results of the first test elution, it was determined that the maximum loading at typical column operating conditions is 45 kg/m^3. As Figure 3 shows, the model accurately predicts the cumulative plutonium discharge with this maximum loading concentration and the particle diffusivity determined from the loading profile analysis.

Figures 4 and 5 compare model predictions with measured rates of discharge of plutonium during both test elutions. A pore diffusivity of 1.0E-10 m^2/s and pore volume fractions of 0.132 prior to desorption of plutonium from the resin and 0.160 after desorption were used to fit the model to the test data. The pore diffusivity is about 100 times greater than reported values for anionic resins.[5] The pore volume fractions correspond to resin bead porosities of 0.198 before desorption and 0.240 after desorption. The porosity increases during desorption due to swelling of the resin and loss of $Pu{\bullet}4NO_3$ by the reaction[5]

$$R_2Pu\left(NO_3\right)_6\,(solid) \Leftrightarrow PuNO_3^{3+} + 3NO_3^{-} + 2RNO_3\,(solid)$$

The solubility for lonac 641™ resin was estimated from eluate plutonium concentrations measured during the first test elution. Before the plutonium concentration spike discharged from the column, the plutonium concentration asymptotically approached a minimum of 0.0106 g/L at a nitric acid concentration of 7850 mol/m^3. The plutonium concentration then rapidly peaked at an apparently constant concentration of 26.3 kg/m^3 at a nominal elution acid concentration of 250 mol/m^3. (The peak concentration was assumed to reach a plateau, because two successive concentrations, measured when 1.03 and 1.54 bed volumes had eluted, were nearly equal.) The most likely explanation for the asymptotic miminum and constant peak concentrations is that the plutonium in the bulk solution was in equilibrium with the adsorbed plutonium on the resin surfaces. Discharge plutonium concentrations should have approached equilibrium levels during this elution because the bulk solution was in contact with partially loaded resin over the entire length of the column.

The lonac 641™ resin equilibrium saturation was estimated by assuming that equilibrium conditions existed for the first test elution. The ratio of the measured equilibrium solubilities for the wash and elution acids was equated to calculated equilibrium values at the measured acid molarities. This calculation yields a solubility constant, K_1, of 0.63 and a saturated equilibrium concentration of 80.6 kg/m^3 at the elution acid concentration of 250 mol/m^3.

It may be noted that the calculated equilibrium concentration is not the same as the maximum measured discharge concentration. One explanation for this apparent contradiction is that the presence of the resin beads does not change the effective cross- sectional flow area. If the cross-sectional area had changed to the fraction occupied by the bulk solution, then. the plutonium would have begun to discharge from the column well before one bed volume had eluted. The plutonium concentration spike does not appear until about one bed volume has eluted, however. This implies that the plutonium travels down the column at the superficial velocity. From a mass balance, it follows that the plutonium discharge concentration is diluted from the actual bulk solution concentration by the ratio of the cross-sectional area occupied by the bulk solution to the total cross-sectional area, i. e., the volume fraction occupied by the bulk solution. If the plutonium concentration in the bulk solution is in saturated equilibrium with the adsorbed resin, then

$$x = \varepsilon_o x_{sat} \quad (46)$$

For x = 26.3 kg/m^3 and x_{sat} = 80.6 kg/m^3,

$$\varepsilon_o = 0.326 \quad (47)$$

This value for the bulk solution volume fraction is slightly less than the value of 0.36 given for random close packing of uniformly sized spheres.[8]

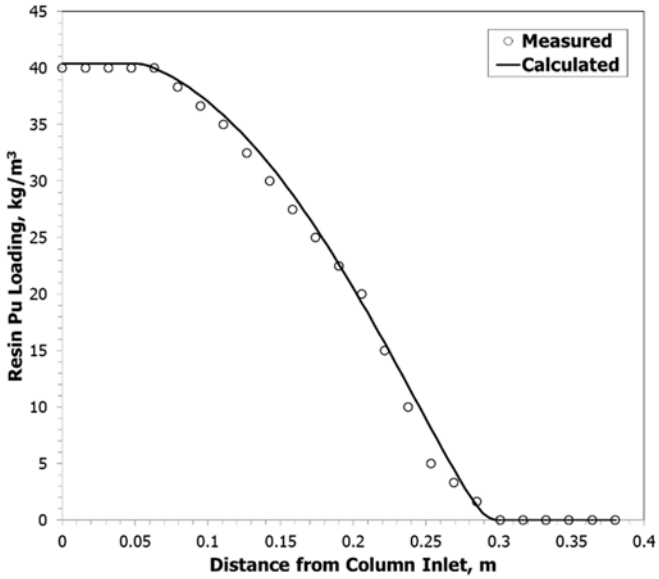

Figure 2. Comparison of Measured and Predicted Resin Loadings after 11 h Wash at 0.0005 m/s with 0.4 kg/m^3 Pu Solution

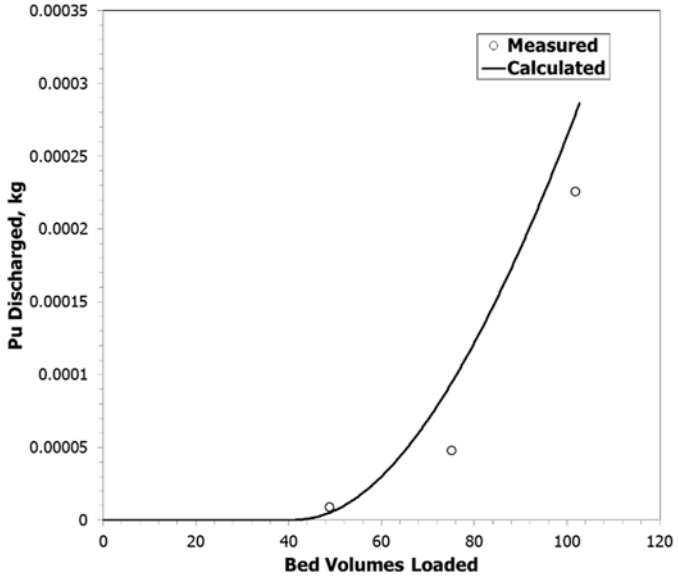

Figure 3. Comparison of Measured and Calculated Cumulative Pu Discharge for First Test Elution (Assumes 45 kg/m^3 Maximum Loading)

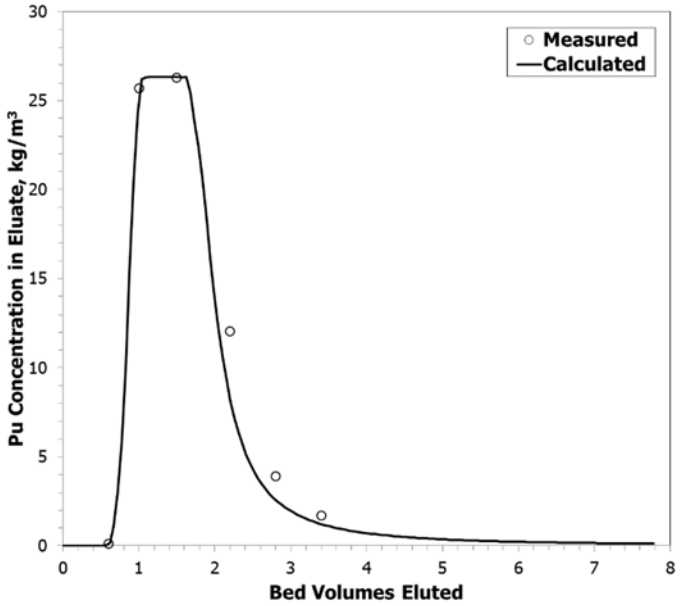

Figure 4. Comparison of Measured and Calculated Elution Profiles for First Test Elution

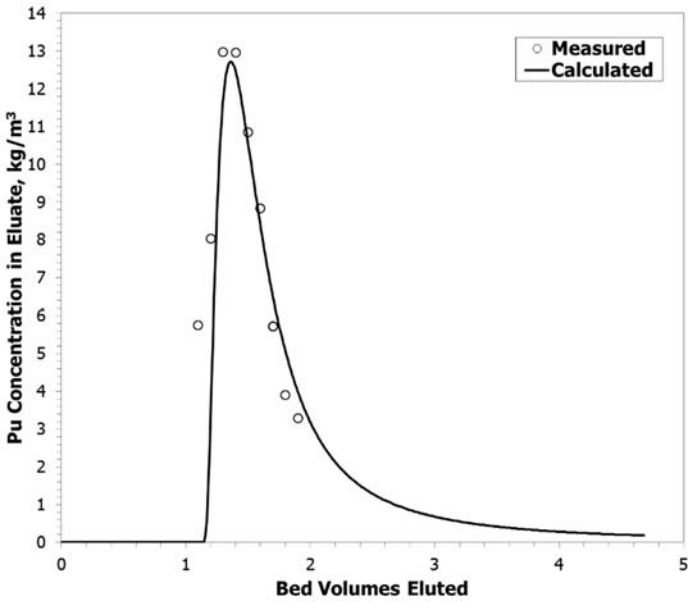

Figure 5. Comparison of Measured and Calculated Elution Profiles for Second Test Elution

Resin Bed Heat Transfer Model

Heat Transfer Model Development

A description of the energy balance used to model heat transfer in the resin bed during flow interruptions follows. The natural convection model includes two-dimensional mass transfer, but that model is not presented. During flow stoppages, if there is a significant plutonium load in the column, most of that plutonium will be adsorbed onto the resin beads, so to a good approximation, the plutonium concentration can be viewed as fixed, and mass transfer by natural convection is of only minor consequence.

The convective heat transfer equation includes a term for the decay heat, Q_{decay}. This equation is

$$\rho_{bed} c_{p,bed} \frac{\partial T}{\partial t} + \rho_f c_{p,f} v_z \frac{\partial T}{\partial z} + \rho_f c_{p,f} v_r \frac{\partial T}{\partial r} = \left(k_{bed} + \rho_f c_{p,f} \alpha_z + \rho_f c_{p,f} D_{mix}\right) \frac{\partial^2 T}{\partial z^2} + \left(k_{bed} + \rho_f c_{p,f} \alpha_r\right) \frac{1}{r} \frac{\partial}{\partial r}\left(r \frac{\partial T}{\partial r}\right) + Q_{decay} C_{Pu} \quad (48)$$

The axial dispersion coefficients in the mass and heat transfer equations is given by Equation 4. The radial dispersion coefficient is about one-fifth as large.[9] Thus,

$$\alpha_r = 0.4 d_p v_z \quad (49)$$

For normal operating conditions (loading, washing, and elution), the superficial axial velocity is specified, and the superficial radial velocity is assumed to be zero. For flow stoppages, these velocities result from natural convection. Natural convection velocities are ignored during loading washing, and elution. At high feed flow rates, the omission of natural convection does not have a significant effect. At lower feed flow rates, this omission is conservative in that it results in higher resin bed temperatures than would be predicted if natural convection were included.

Velocity components for natural convection flow are calculated by combining the Ergun equation with axial and radial component momentum equations, as suggested by Stewart and Dona.[10] The axial velocity for natural convection is modeled using a form of the Ergun equation for laminar flow, which is[11,12]

$$v_z = \frac{d_p{}^2 \varepsilon_o{}^4 \left(\rho - \bar{\rho}\right) g}{200 \left(1 - \varepsilon_o\right)^2 \mu} \quad (50)$$

It may be noted that in Equation 54, $v_z \propto \frac{\varepsilon_o{}^4}{1 - \varepsilon_o{}^2}$, while in the Ergun equation, $v_z \propto \frac{\varepsilon_o{}^3}{1 - \varepsilon_o{}^2}$. The extra void fraction multiplier is added because the buoyant force applies only to the fraction of the total volume occupied by the bulk solution and not to the resin beads.

The Ergun equation was originally derived for unidirectional flow. To model the two-dimensional flow in the resin bed, separate equations are used for the axial and radial velocity components. These equations take the form

$$v_z = \frac{d_p{}^2 \varepsilon_o{}^4}{200 \left(1 - \varepsilon_o\right)^2 \mu} \left(-\frac{\partial P}{\partial z} + \left(\rho_f - \bar{\rho}_f\right) g\right) \quad (51)$$

and

$$v_r = \frac{{d_p}^2 {\varepsilon_o}^4}{200\left(1-\varepsilon_o\right)^2 \mu}\left(-\frac{\partial P}{\partial r}\right) \tag{52}$$

The buoyancy term in the axial velocity equation contains a reference density, $\bar{\rho}$. At equilibrium, the reference density must be set so that there is no net flow upward or downward at any bed level. This implies that the reference density must equal the average fluid density at a given bed level. In other words,

$$\bar{\rho}_f = \frac{2}{R^2}\int_{r=0}^{R} r\,\rho_f\,dr \tag{53}$$

The pressure gradient terms must be eliminated from Equations 17 and 18 to solve for the velocity components. This is accomplished by taking cross derivatives. The resulting equation is

$$\frac{\partial v_r}{\partial z} - \frac{\partial v_z}{\partial r} + \frac{{d_p}^2 {\varepsilon_o}^4 g}{200\left(1-\varepsilon_o\right)^2 \mu}\frac{\partial \rho_f}{\partial r} = 0 \tag{54}$$

The radial velocity is calculated by combining the continuity relation,

$$\frac{1}{r}\frac{\partial r v_r}{\partial r} + \frac{\partial v_z}{\partial z} = 0 \tag{55}$$

with Equation 54.

The natural convection velocities defined by Equations 55 and 56 do not account for convection due to cross-sectional average axial density gradients. At the start of a flow stoppage, the solution in the resin bed is unstably stratified, with the higher plutonium concentrations and therefore the higher densities at the top of the resin bed. Preliminary calculations with these velocities showed that the solution remained unstably stratified even as equilibrium approached. Actually, significant unstable axial density variations would cause heavier fluid from above to mix with lighter fluid from below in regularly spaced regions called Bénard cells. A detailed model of Bénard cell convection was not attempted. Instead, mixing due to axial density gradients is calculated using an analogy to bubble columns. A dispersion model is used to describe mixing in bubble columns. The dispersion coefficient for bubble columns is defined in terms of the circulation velocity induced by the bubble motion, v_c, and the column diameter:[13]

$$D_{mix} = 0.24\,d\,v_c \tag{56}$$

The same correlation is used to calculate the dispersion due to buoyancy-induced mixing in the resin bed. The circulation velocity is set equal to half that given by the Ergun equation and the pressure gradient based on the difference between the average densities for different levels:

$$v_c = \frac{{d_p}^2 {\varepsilon_o}^4 \left(\bar{\rho}_f\big|_z - \bar{\rho}_f\big|_{z+\Delta z}\right) g}{400\left(1-\varepsilon_o\right)^2 \mu} \tag{57}$$

The one-half factor appears because mixing occurs in both directions and can therefore occupy only half of the cross-sectional flow area in either direction. The use of cross-sectional average densities accounts for the axial pressure gradients neglected by Equation 51. That equation already incorporates local density variations in the radial direction, so local density gradients are not included.

In the model, the dispersion coefficient is calculated using a weighted distribution of circulation velocities for density differences at different levels. The distribution is based on the

mixing height for the dispersion coefficient, which is 0.8 times the column diameter.[13] If it is assumed that the mixing intensity decreases exponentially with axial distance, these values for the mixing height and velocity give the following expression for the local mixing velocity:

$$v_{c,eff} = v_c \exp\left(-2 \frac{|z - z_0|}{0.8d} \right) \quad (58)$$

where z_0 is the axial location at which the dispersion coefficient is evaluated. It can be confirmed that an integration of this equation with respect to axial displacement gives the mixing height.

Boundary Conditions for Heat Transfer

The solution of the energy equation required boundary conditions for thermal conduction and inlet conditions for natural convection. Mass balances for loading, washing, and elution provided the initial conditions when flow is interrupted.

Two conditions were specified for the LANL column, exposure to ambient air and cooling by a water jacket. For air exposure, the conduction of heat from the resin bed through the circumferential wall equals the combined rate of natural and forced convection and thermal radiation to the ambient air. For thermal radiation, a value of 0.6 was used for the surface emissivity ε. This emissivity is characteristic for steel surfaces and is a conservatively low estimate for glass surfaces.[14] Standard Nusselt number correlations were used to model natural convection[15] and forced convection.[16] For cooling by a water jacket, it was assumed that the wall temperature equals the water temperature. It was assumed that there is no heat transfer at the top and bottom of the column.

Inlet and outlet flow conditions were specified by assuming that the fluid exiting the resin bed due to natural convection becomes well-mixed in small volumes of free-standing liquid above and below the bed.

Calculation Method for Natural Convection Calculations

A forward time step, donor cell finite difference method was used to model the natural convection heat transfer. The flow terms in the heat transfer equations were expressed in terms of a stream function. Time step sizes of 0.02 s for operation at the specified feed flow rate and 1.0 s for natural convection during flow stoppages were used. Cell sizes were decreased until approximate convergence of temperature profiles and flow streamlines was obtained. It was determined that a grid of 48 axial cells by 24 radial cells gave an adequate approximation.

Results of Natural Convection Heat Transfer Calculations

Figure 6 depicts the effect of a flow stoppage on the maximum resin bed temperature for the 0.0746-m diameter by 0.341-m tall LANL column. This figure shows results for a case where the column would be inadvertently fed twice its capacity of 0.05 kg Pu-238. During a flow stoppage, the maximum column temperature would increase from 331 K to 358 K if the column were air cooled and from 318 K to 335 K if the column were cooled by a water jacket. Even for air cooling, the temperature remains well below the 388 K minimum temperature for initiation of a reaction excursion, so no water jacket is needed.

Figures 7 and 8 illustrate the temperature profile and the recirculation streamlines for natural convection for the air cooling case from Figure 6. The streamlines in Figure 8 demonstrate that there are two circulation cells, one in the top portion of the column and one in the bottom portion.

Within both cells, the flow is upward near the column centerline and downward along the column wall. The top cell is slightly stronger than the bottom cell, so temperatures in the bottom of the column slightly exceed the temperatures in the top of the column.

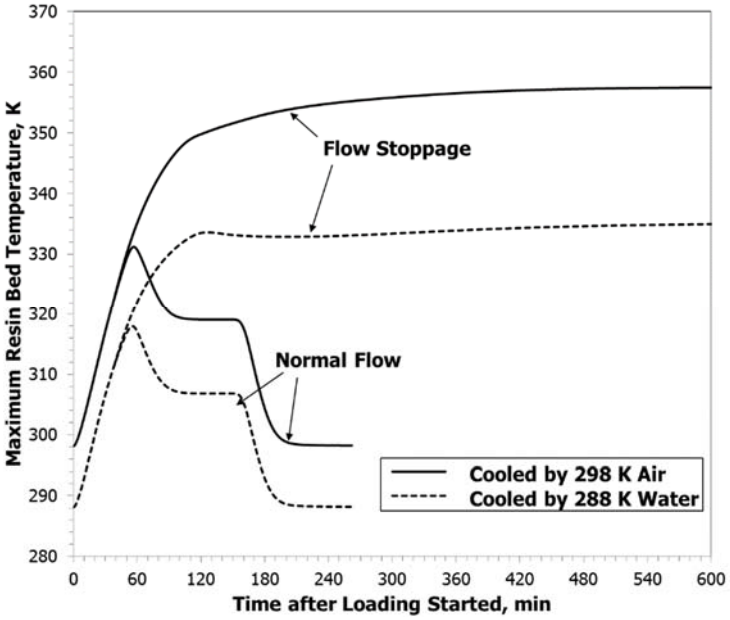

Figure 6. Maximum Resin Bed Temperatures for a Low Feed Flow Rate, High Feed Concentration, with Twice the Resin Capacity Fed

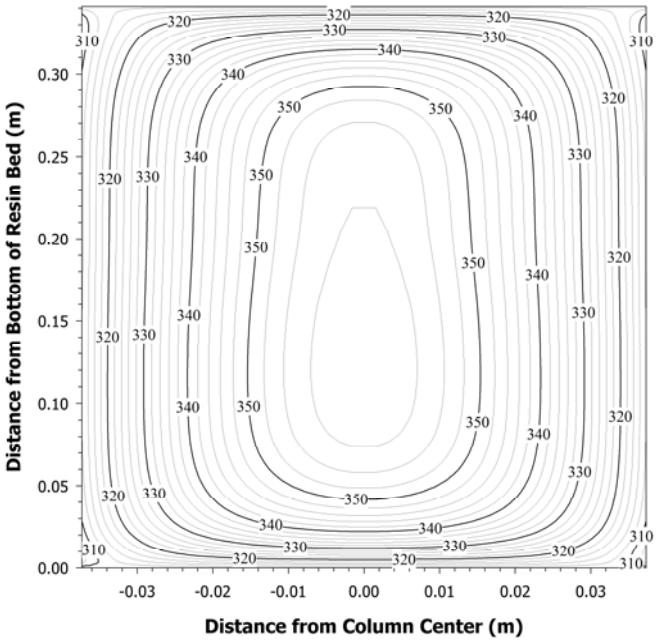

Figure 7. Temperature Distribution at Thermal Equilibrium after a Flow Stoppage for Low Feed Flow Rate, High Feed Concentration, Exposure to 298 K Air, and Twice the Resin Capacity Fed

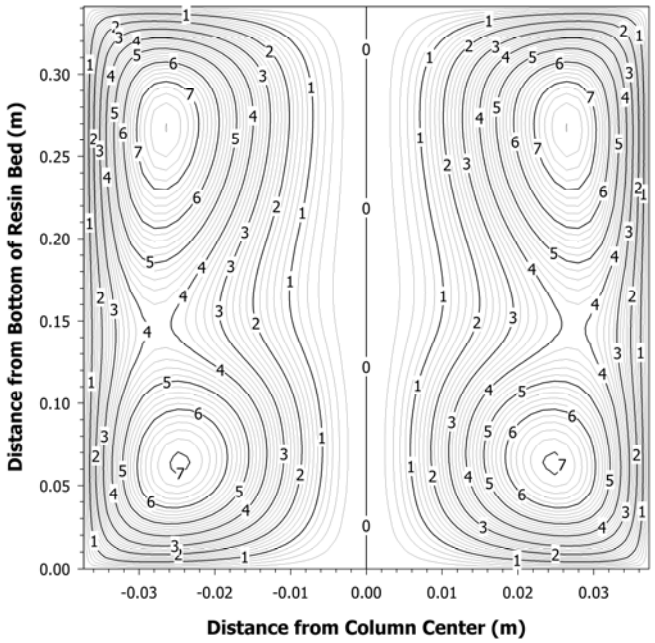

Figure 8. Flow Streamlines at Thermal Equilibrium after a Flow Stoppage for Low Feed Flow Rate, High Feed Concentration, Exposure to 298 K Air, and Twice the Resin Capacity Fed (Numbers on graph are values of the stream function in 1E-7 m^2/s.)

Resin Dose Calculations

Impact of Resin Dose on Ion Exchange Column Safety and Performance

Recently, the resin bed model was used to estimated doses to the resin for purification of plutonium in a 0.015-m diameter, 0.5-m tall column containing Reillex HPQ™ resin. The feed stream to the ion exchange column was to contain plutonium with a mixed isotope distribution, contaminated with the principal radioactive isotopes Am-243, Cm-244, Cs-137, and Sr-90. (The cesium and strontium are present as fission products.) The ion exchange column purifies the feed stream by preferentially adsorbing the plutonium. The distribution coefficient for the preferential adsorption of plutonium relative to americium and curium was estimated to be 165, based on laboratory tests.[17] The resin does not adsorb cesium or strontium to any significant extent.

During the ion exchange column operation, irradiation from adsorbed and non-adsorbed radionuclides decreases the exchange capacity of the resin and makes it more susceptible to attack by the nitric acid in the loading and washing solutions. At high temperatures, the nitric acid-resin decomposition reactions are exothermic and self-accelerating. These reactions pose a safety risk because they release product gases that can pressurize the ion exchange column.

In SRNL thermal degradation tests, rates of heating and pressurization did not change significantly for resin exposed to a 3E6 Gy dose but exhibited significant changes for a dose of 5E6 Gy. Previous tests conducted at Los Alamos National Laboratory (LANL) demonstrated that the plutonium adsorption capacity of the resin decreased by 10% or less for a dose of 3E6 Gy.[18] Based on these results, the recommended maximum radiation dose for the Reillex HPQ™ resin was set at 3E6 Gy.

Resin Dose Model

The total dose to the resin was calculated as the sum of the doses from individual radioactive isotopes. Doses are based on the residence time of each isotope in the column.

The dose analysis accounts for partial shielding of the resin from alpha radiation by the acid solution in the column. This shielding is evaluated in terms of the travel distance of an alpha particle in solution. The alpha particle travel distance is correlated in terms of the atomic number of the medium containing the alpha particle, the particle energy, and the absorber material density.[19] It has been determined that, if the alpha particles travel a uniform distance and lose energy at a constant rate along their travel paths, all particles generated within one travel path distance of a solid surface will transmit, on average, one-eighth of their energy to the solid.[20] Consequently, the resin beads are subject to alpha radiation only from solution within one travel path distance of their surfaces, and within that range, the beads only adsorb one-eighth of the total alpha energy. It is conservatively assumed that all beta and gamma radiation penetrates the beads and is deposited in the column.

Dose Calculation Results

Figure 9 depicts the dose profile at the end of the feeding and elution stage. At the end of elution, the total cumulative dose at the top of the column is 8170 Gy, well below the limiting dose of 3E6 Gy. Slightly less than half the maximum dose is from plutonium, and slightly more than half the maximum dose is from curium. The plutonium dose is primarily from the plutonium that adsorbs onto the resin, and the curium dose is mostly from curium that passed through the column during the feeding stage. Americium, cesium, and strontium contribute only slightly to the total dose.

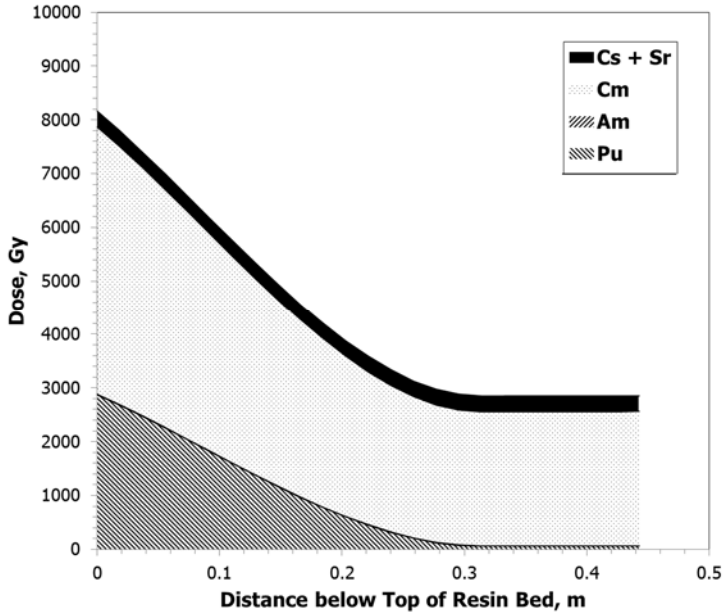

Figure 9. Cumulative Dose on Column after Elution

Conclusions

A finite element code has been developed to model mass and heat transfer in anion exchange columns used to extract plutonium. The model is applied to model unidirectional forced flow during normal column operations and natural convection during flow stoppages. Resin loading is modeled by combining a chemical equilibrium absorption relation with models for axial dispersion and solid phase diffusion. Elution is modeled by combining the axial dispersion model with a shrinking core diffusion model. Natural convection calculations are based on the Ergun relation for flow in a packed bed. The model treats the resin bed as a continuum so that a regular axisymmetric calculation grid can be used, without any fine discretization to accommodate boundary layers. As a consequence, the code is computationally efficient.

Calculations demonstrate that the code can accurately model loading profiles and elution transients for typical plutonium extraction operations. Examples are presented for the modeling of natural convection during a flow stoppage and for calculation of the radiolytic dose to the resin for an extraction cycle.

Acknowledgment

This manuscript has been authored by Savannah River Nuclear Solutions, LLC under Contract No. DE-AC09-08SR22470 with the U.S. Department of Energy. The United States Government retains and the publisher, by accepting the article for publication, acknowledges that the United States Government retains a non-exclusive, paid-up, irrevocable, world-wide license to publish or reproduce the published form of this manuscript, or allow others to do so, for United States Government purposes.

Partial funding for this work was provided by Los Alamos National Laboratory.

References

1. Laurinat, J.E., "Self-Heating of Pu-238 Anion Exchange Column (U)," Westinghouse Savannah River Company Report No. WSRC-TR-94-0166, March 1994.
2. Laurinat, J.E., "Thermal Analysis of LANL Ion Exchange Column," Westinghouse Savannah River Company Report No. WSRC-TR-99-00027, May 1999.
3. Pansoy-Hjelvik, M.E., J.Z. Nixon, J. Laurinat, J. Brock, G. Silver, M.A. Reimus, and K.B. Ramsey, "Process Parameters Optimization in Ion Exchange ^{238}Pu Aqueous Processing," Los Alamos National Laboratory Report No. LA-UR-00-1546, presented at Plutonium Futures – The Science Conference, Santa Fe, NM, July 10-13, 2000.
4. Laurinat, J.E., "Revised Thermal Analysis of LANL Ion Exchange Column," Westinghouse Savannah River Company Report No. WSRC-TR-2006-00123, April 2006.
5. Ryan, J.L. and E.J. Wheelwright, "The Recovery, Concentration, and Purification of Plutonium by Anion Exchange in Nitric Acid," General Electric-Hanford Atomic Products Operation Report HW-55893, January 1959.
6. Perry's Chemical Engineers' Handbook, 6th ed., D.W. Green, ed., McGraw-Hill, New York (1984), p. 16-27.
7. Vermeulen, T., "Theory for Irreversible and Constant-Pattern Solid Diffusion," Ind. Eng. Chem., 45(8), 1664-1670, 1953.
8. Dullen, F.A.L., Porous Media: Fluid Transport and Pore Structure, 2nd ed., Academic Press, San Diego, California (1992).
9. Ebach, E.A. and R.R. White, "Mixing of Fluids Flowing through Beds of Packed Solids," A.I.Ch.E. J., 4(2), 161-169.
10. Stewart, Jr., W.E. and C.L.G. Dona, "Free Convection in a Heat Generating Porous Medium in a Finite Vertical Cylinder," J. Heat Transfer, 110(2), 1988, 517-520.
11. Perry's Chemical Engineers' Handbook, 6th ed., D.W. Green, ed., McGraw-Hill, New York (1984), p. 5-54.
12. Leva, M., Fluidization, McGraw-Hill, New York (1959), p. 47.
13. Joshi, J.B., "Axial Mixing in Multiphase Contactors – A Unified Correlation," Trans. I. Chem. E., 58, 155-165, 1980.
14. Perry's Chemical Engineers' Handbook, 6th ed., D.W. Green, ed., McGraw Hill, New York (1984), p. 10-51.
15. Perry's Chemical Engineers' Handbook, 6th ed., D.W. Green, ed., McGraw Hill, New York (1984), p. 10-13.
16. Kreith, F. and W.Z. Black, Basic Heat Transfer, Harper and Row, New York (1980), p. 251.
17. Kyser III, E.A. and W.D. King, "HB-Line Anion Exchange Purification of AFS-2 Plutonium for MOX," SRNL Report SRNL-STI-2012-00233, Rev. 1, July 2012.
18. Marsh, S.F., "The Effects of In Situ Alpha-Particle Irradiations on Six Strong Base Anion Exchange Resins," LANL Report LA-12055, April 1991.
19. Friedlander, G., J.W. Kennedy, and J.M. Miller, Nuclear and Radiochemistry, 2nd ed., John Wiley & Sons, New York (1949), p. 95.
20. Laurinat, J.E., N.M. Askew, and S.J. Hensel, "Flammability Analysis for Actinide Oxides Packaged in 9975 Shipping Containers," Paper PVP2013-97478, Proceedings of the 2013 ASME Pressure Vessels & Piping Conference, Paris, France, July 14-18, 2013.